sustainability

MDPI

Article

Summer Sea-Surface Temperatures and Climatic Events in Vaigat Strait, West Greenland, during the Last 5000 Years

Dongling Li [1,*], Longbin Sha [1], Jialin Li [1,2], Hui Jiang [3], Yanguang Liu [4] and Yanni Wu [1]

1 Department of Geography & Spatial Information Techniques, Ningbo University, Ningbo 315211, China; shalongbin@nbu.edu.cn (L.S.); lijialin@nbu.edu.cn (J.L.); wuyanni_1124@163.com (Y.W.)
2 Research Center for Marine Culture and Economy, Ningbo 315211, China
3 Key Laboratory of Geographic Information Science, East China Normal University, Shanghai 200062, China; hjiang@geo.ecnu.edu.cn
4 Key Laboratory of Marine Sedimentology and Environmental Geology, First Institute of Oceanography, State Oceanic Administration, Qingdao 266061, China; yanguangliu@fio.org.cn
* Correspondence: lidongling@nbu.edu.cn; Tel.: +86-574-87609516

Academic Editor: Vincenzo Torretta
Received: 19 February 2017; Accepted: 25 April 2017; Published: 28 April 2017

Abstract: We present a new reconstruction of summer sea-surface temperature (SST) variations over the past 5000 years based on a diatom record from gravity core DA06-139G, from Vaigat Strait in Disko Bugt, West Greenland. Summer SST varied from 1.4 to 5 °C, and the record exhibits an overall decreasing temperature trend. Relatively high summer SST occurred prior to 3000 cal. a BP, representing the end of the Holocene Thermal Maximum. After the beginning of the "Neoglaciation" at approximately 3000 cal. a BP, Vaigat Strait experienced several hydrographical changes that were closely related to the general climatic and oceanographic evolution of the North Atlantic region. Distinct increases in summer SST in Vaigat Strait occurred from 2000 to 1600 cal. a BP and from 1200 to 630 cal. a BP, and are consistent with the "Roman Warm Period" and the "Mediaeval Warm Period" in the North Atlantic region. The summer SST decreased significantly during 1500~1200 cal. a BP and 630~50 cal. a BP, corresponding, respectively, to the Northeast Atlantic cooling episodes known as the "European Dark Ages" and "Little Ice Age". Spectral and cross-correlation analyses indicate that centennial-scale oscillations in summer SST are superimposed on the long-term trend. The dominant periodicities are centered at 529, 410, and 191 years, which are close to the ubiquitous 512 and 206-year ^{14}C cycle, suggesting that solar forcing may play an important role in summer SST variability in Disko Bugt.

Keywords: diatoms; sea-surface temperature; transfer function; West Greenland; Holocene

1. Introduction

The Disko Bugt area in central West Greenland has attracted considerable research attention in recent years, and there have been studies of both oceanic variability [1–4] and fluctuations in tidewater-based ice streams such as Jakobshavns Isbrae [5–9]. In addition, special attention has been paid to the variation of the ice sheet and the deglaciation during the late Quaternary, and to the nearshore-to-offshore ocean circulation during the Holocene. The hydrography of the coastal waters of West Greenland is linked to the large-scale North Atlantic circulation system via the combined effects of the East Greenland Current (EGC) and the Irminger Current (IC), which merge to form the West Greenland Current (WGC; Figure 1). Thus, summer sea-surface temperatures (SSTs) off West Greenland are largely determined by the relative flow of Polar and Atlantic water masses within the WGC. Multi-proxy reconstructions of SST along West Greenland have so far mainly been

qualitative [2,4,10,11]. However, quantitative SST reconstructions on a long timescale are necessary to help understand the dynamics of the ocean-climate system.

Various proxies have been used to reconstruct palaeoclimatic and palaeoceanographic changes in the northern North Atlantic [12–24]. Among these, diatoms are a common and abundant component of Arctic phytoplankton communities, and their distribution is strongly influenced by surface water temperature and sea ice cover [25–27]. In the North Atlantic region, diatoms have been used as a tool for quantitative reconstructions of summer SST and sea ice concentration (SIC) during the Holocene using the transfer function method [22–24,28–30]. However, except for the reconstructions of SIC by Sha et al. [17] and of SST and SIC by Krawczyk et al. [31], there is a dearth of diatom-based reconstructions from West Greenland.

The Sun is the main driver of Earth's climate [32], and several studies have demonstrated that the effect of solar changes on regional modes of atmospheric variability is evident in the instrumental record [33–35]. Solar activity has been proposed to influence variability in various components of the climate system, such as temperature, winds, precipitation, and drift ice [15,18,36–41]. For example, Bond et al. [41] found that Holocene drift ice in the North Atlantic and records of the cosmogenic nuclides ^{10}Be and ^{14}C are correlated, and concluded that variations in solar activity may have played a significant role in iceberg production and drift. Holzhauser et al. [42] found that glacier advances and lake level changes are correlative with increased ^{14}C production rate (reduced solar activity). Furthermore, changes in SST reconstructions also exhibit very similar patterns to variations in solar activity. The strong correlation of the Norwegian Sea temperature with solar activity over the last millennium indicates that variations in solar activity affect regional atmospheric variability, which in turn controls the poleward transport and temperature of warm Atlantic surface waters [43].

Here, we present a diatom-based summer SST record from a marine sediment core (gravity core DA06-139G) from Vaigat Strait, Disko Bugt, central West Greenland. Our objectives are twofold: firstly, to quantitatively reconstruct summer SSTs over the past 5000 years in Vaigat Strait; and secondly, to assess potential forcing mechanisms of summer SST variability.

2. Oceanographic Setting

Disko Bugt is a large marine embayment (68°30′–69°15′N, 50°00′–54°00′W; Figure 1) in central West Greenland. Water depths generally range from 200 to 400 m, but reach 990 m in the deep submarine valley Egedesminde Dyb, which extends in a south-westerly direction [44].

Vaigat Strait is situated to the north of Disko Bugt (Figure 1B), and is bound by Disko Island to the southwest and by the Greenland mainland to the northeast. It acts as a major exit pathway for the WGC waters entering Disko Bugt, as well as for meltwater and icebergs generated by the major tidewater glaciers, including the Jacobshavn Isbræ, northwards into Baffin Bay [44,45]. The strait is ca. 130 km long and 20–25 km wide, and has a maximum water depth of ~600 m [45]. It is suggested that the passage acted as a northern conduit of an ice lobe extending to the mouth of the strait during the last glaciation [46].

The surface circulation to the west of Greenland and adjacent areas is dominated by two major currents: the WGC, which flows northwards along the west coast of Greenland, and the Baffin–Labrador Current (BLC) which flows southwards along the east coast of Baffin Island and Labrador (Figure 1A). The WGC consists of a combination of (i) Arctic-sourced cold, low-salinity water from the EGC (at 0–200 m water depth), designated Polar water [47]; and (ii) relatively warm and saline Atlantic-sourced water from the IC (>200 m water depth), a branch of the North Atlantic Current (NAC, [47,48]). The two components mix continuously as the WGC flows northwards, but can still be distinguished to the southwest of Disko Bugt [49].

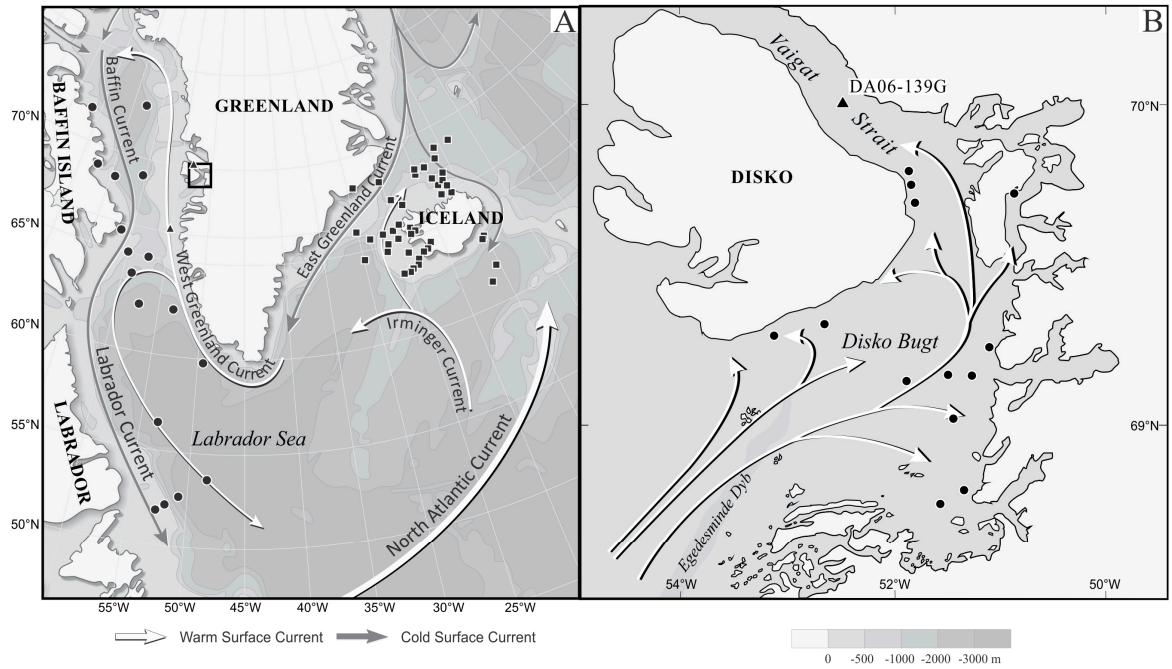

Figure 1. (**A**) Surface circulation in the NW Atlantic and locations of diatom samples in the study area. (**B**) Enlargement of the study area, indicated by the square in Figure 1A. Filled circles indicate new samples from off West Greenland. Filled squares represent samples from off East Greenland and Iceland previously published by Jiang et al. [15]. Figure modified from Sha et al. [17].

3. Materials and Methods

3.1. Palaeo-Records: Sediment Cores and Diatom Samples

A 446-cm-long gravity core, DA06-139G (Figure 1B), was collected from Vaigat Strait in Disko Bugt at 70°05.486′N, 52°53.585′W (water depth 384 m) during a cruise of the Danish research vessel "Dana" in 2006 [50]. Further information about the core is given in Andresen et al. [45]. A total of 90 samples (a 1-cm sediment sample taken every 5 cm) from core DA06-139G were analysed for their diatom content.

Sample preparation following the methods of Håkansson [51] and Sha et al. [17]. A minimum of 300 diatom valves were counted in random transects for each sample (excluding *Chaetoceros* resting spores, cf. [52,53]). Diatom percentages were calculated based on the diatom sum, excluding *Chaetoceros* resting spores.

3.2. Age Model for the Sediment Core

The chronology for core DA06-139G is based on 10 AMS (Accelerator Mass Spectrometry) ^{14}C dates from molluscs, marine plant (sea grass) fragments, and one sample of mixed benthic foraminifera. All ^{14}C ages are calibrated with the OxCal 4.1 software [54] using theMarine09 calibration data set [55] with a local marine reservoir age ΔR of 140 $\pm$ 30 [56,57]. An age model was obtained using the depositional model option in OxCal with a *k* value of 100, which produced A_{model} = 52.0% (Figure 2).

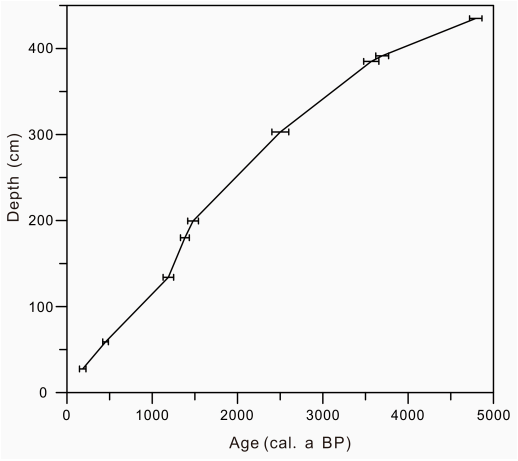

Figure 2. Age–depth model for gravity core DA06–139G from Vaigat Strait, Disko Bugt, West Greenland.

3.3. Modern Diatom Data Set and Diatom-Based Transfer Function

A modern enlarged data set of diatoms and environmental variables—mainly from coastal waters around Iceland, with some sites from off Greenland—was used to produce a diatom-based transfer function for quantitative reconstruction of summer SST. The data set includes 30 surface samples taken from West Greenland during a cruise of the Danish research vessel "Porsild" in 1999 and the German research vessel "Maria S. Merian" in 2008. To increase the temperature range, 50 surface samples from east of Greenland and from around Iceland which have been successfully used in quantitative diatom-based summer SST reconstruction from the northern North Atlantic [15,16,19] were also included in the modern data set [28]. In total, surface sediment diatom data from 80 surface samples were used in the new modern data set (see Supplementary Table S1).

The computer program C2 [58] was used to quantitatively reconstruct summer SST. Seven numerical reconstruction methods were assessed to define the optimal diatom-based summer SST transfer function (Table 1). The weighted averaging partial least squares (WA-PLS) method with two components resulted in a low root-mean-squared error of prediction ($RMSEP_{(Jack)}$) (1.393), a low maximum bias (2.047), and a high squared correlation ($R^2_{(Jack)}$) (0.853) (Table 1). In addition, a plot of jack-knife-inferred SST versus observed SST exhibits a strong linear correlation (Figure 3A), and the residuals are randomly scattered (Figure 3B). Thus, the WA-PLS with two components was used to estimate summer SST variability in Disko Bugt, West Greenland. The prediction error for each fossil sample—which combines the standard error of estimates for each sample with the error in the calibration function—was calculated using the program C2.

Table 1. Results of testing the methodology for constructing the transfer function. Root-mean squared errors (RMSE), root mean squared error of prediction based on leave-one out jack-knifing ($RMSEP_{(Jack)}$), Max_Bias and R^2 for reconstructed summer sea-surface temperature (SST, °C) in seven reconstruction procedures. WA = weighted averaging, $WA_{(tol)}$ = weighted averaging with tolerance down-weighting, PLS = partial least squares, WA-PLS = weighted averaging partial least squares, and MAT = modern analogue technique. Both inverse and classical deshrinking regression were used in WA and $WA_{(tol)}$ reconstruction procedures. The results demonstrated that WA-PLS with two components is the most reliable (values in bold).

		Max_Bias	**$R^2_{(Jack)}$**	**$RMSEP_{(Jack)}$**
WA	Inverse	2.539	0.836	1.471
$WA_{(tol)}$	Inverse	3.420	0.796	1.638
WA	Classical	1.932	0.837	1.538
$WA_{(tol)}$	Classical	2.942	0.797	1.716

Table 1. *Cont.*

		Max_Bias	$R^2_{(Jack)}$	$RMSEP_{(Jack)}$
PLS	1 component	2.376	0.641	2.173
PLS	2 components	2.904	0.765	1.759
PLS	3 components	2.897	0.796	1.641
PLS	4 components	2.694	0.819	1.543
PLS	5 components	2.412	0.841	1.444
WA-PLS	1 component	2.540	0.836	1.470
WA-PLS	2 components	**2.047**	**0.853**	**1.393**
WA-PLS	3 components	2.201	0.860	1.355
WA-PLS	4 components	2.072	0.862	1.346
WA-PLS	5 components	2.084	0.855	1.383
MAT	1 analogue	2.740	0.816	1.610
MAT	2 analogues	1.720	0.852	1.443
MAT	3 analogues	2.280	0.845	1.467
MAT	4 analogues	2.555	0.849	1.452
MAT	5 analogues	2.460	0.841	1.489

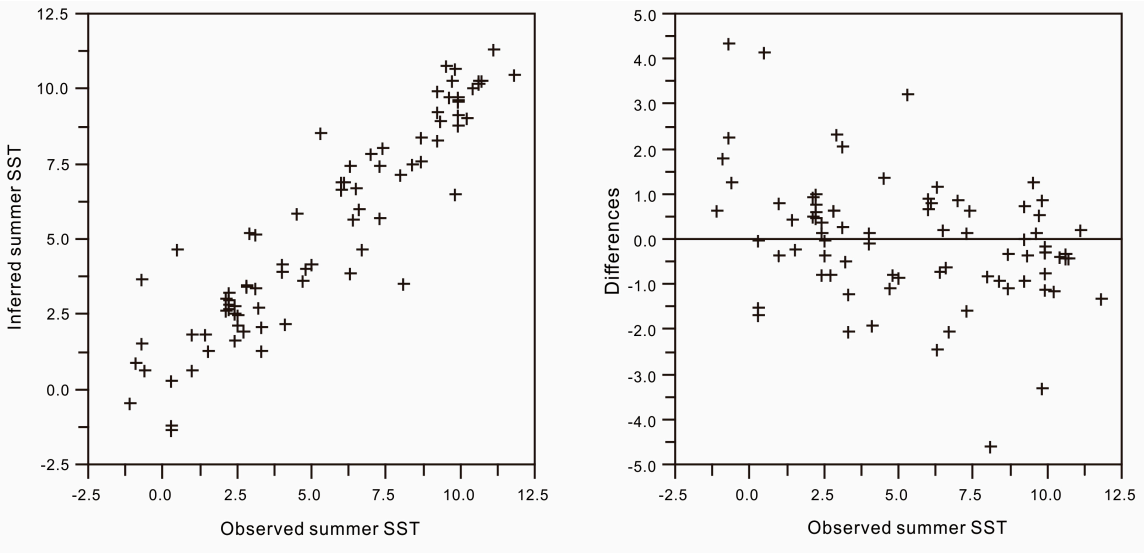

Figure 3. Plots of (**A**) jack-knife-inferred SST using WA-PLS (two components) versus observed SST (°C) and (**B**) of the differences between jack-knife inferred and observed SSTs versus observed SST (°C).

3.4. Statistical Analysis

The power spectrum of the reconstructed summer SST record was calculated using the publicly available REDFIT software [59], which applies the Lomb–Scargle Fourier transform [59]. The Lomb–Scargle method is based on a least-squares fit of sinusoids to the time series data. The univariate spectra were bias-corrected using 1000 Monte-Carlo simulations. REDFIT automatically produces first-order autoregressive (AR1) time series with sampling times and characteristic time scales that match those of the actual climate data. To test the statistical significance of an individual spectral peak, REDFIT estimates the upper confidence interval of the AR1 noise for various significance levels based on a x^2 distribution. To reveal the general physical-phase correlations between the reconstructed summer SST record and total solar irradiance (TSI), cross-correlation analysis of the two records was undertaken using the Arand software package [60].

4. Results

The reconstructed summer SSTs ranged from 1.4 to 5 °C, with a mean of 3.1 °C; in addition, a long-term cooling trend of the water masses in Vaigat Strait is evident during the past 5000 years (Figure 4A). The summer SSTs were generally higher than the mean value before 3000 cal. a BP, except for short intervals of somewhat low summer SST between 4800 and 5000 cal. a BP. Subsequently, there was a gradual decrease in the reconstructed summer SST after 3000 cal. a BP which continued until about 2000 cal. a BP. A warm interval, centered at about 1700 cal. a BP was succeeded by decreasing SSTs, which reached their lowest values at about 1500 cal. a BP. There was a gradual increase in reconstructed summer SST during the interval from 1200 to 630 cal. a BP, followed by a distinct decrease after 630 cal. a BP. The prediction error for each sample ranges between 0.278 and 1.727 °C.

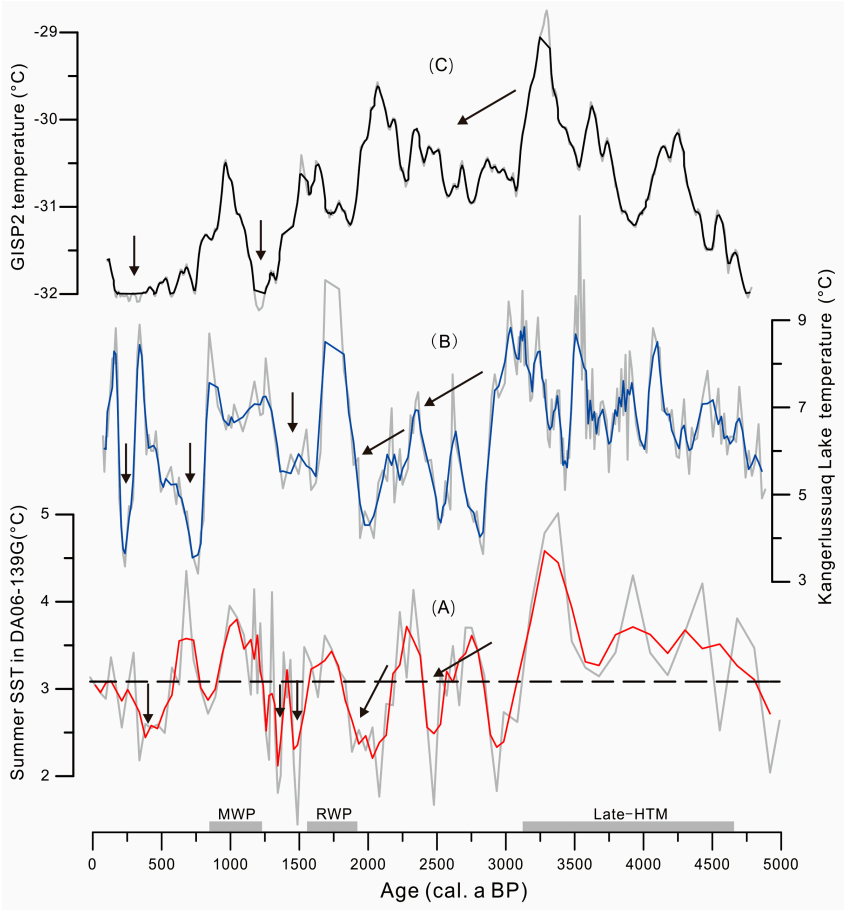

Figure 4. (**A**) Diatom-based reconstructed summer SST record for core DA06-139G. (**B**) Temperature records based on alkenone unsaturation from Lake E in Kangerlussuaq, West Greenland [61] (**C**) Temperature reconstruction from the GISP2 ice core, Summit, Greenland [62]. Actual data are shown as grey lines; smoothed records (three-point running means) are denoted by coloured lines. The dashed line is the mean value. Historical NE Atlantic climate events are indicated at the bottom of the diagram. Arrows indicate intervals with decreased reconstructed temperature.

Spectral analysis of the record reveals statistically significant (above the 90% confidence level), centennial-scale periodicities centered at 529, 410, 191, 131, 124, and 114 years (Figure 5). The 529, 410, and 191-year periodicities are close to the ubiquitous 512 and 206-year ^{14}C cycles [63], which indicates that solar modulation may play a role in driving centennial-scale variations in SST in Vaigat Strait. However, the periodicities of ~114–131 years should be regarded as uncertain, because they are too close to the Nyquist frequency.

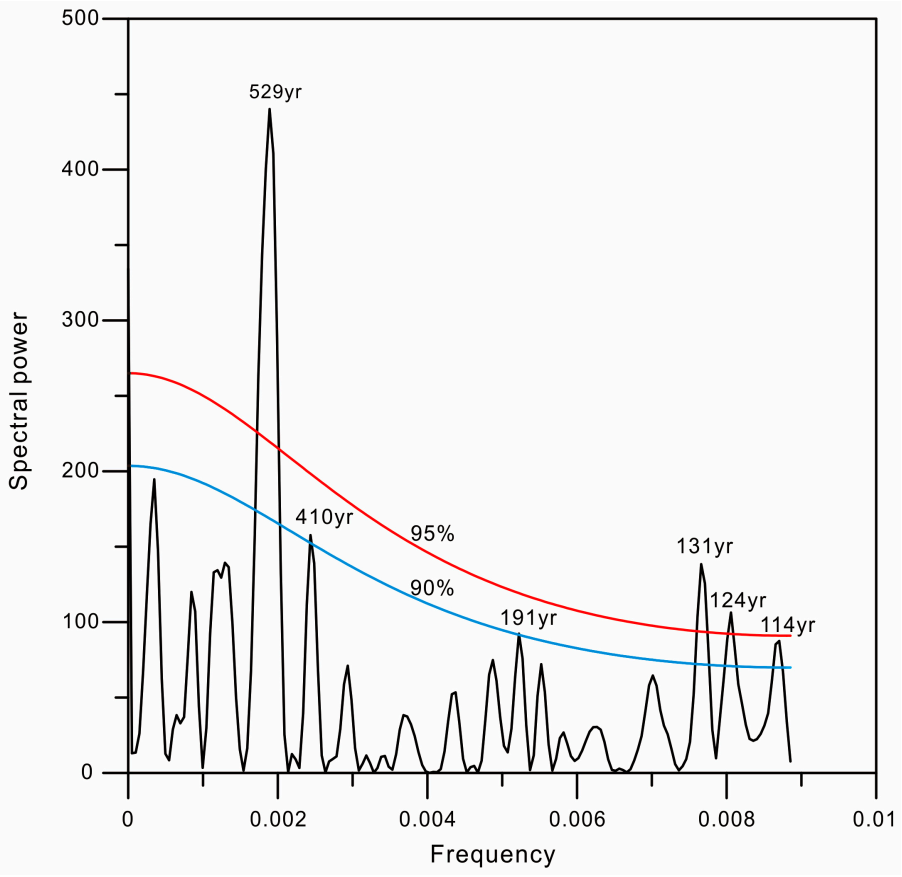

Figure 5. Results of spectral analysis of the reconstructed summer SST record from core DA06-139G. The black lines indicate the 95% (red), and 90% (blue) red-noise false-alarm levels. Notable peaks occur at 529, 410, 191, 131, 124, and 114 years. Peaks at ~114–131 years and below are too close to the Nyquist frequency to be reliable.

5. Discussion

5.1. 5000–3000 cal. a BP: Late-Holocene Thermal Maximum

The summer SST record of the last 5000 years from core DA06-139G reflects the interactions of different water masses, each with its own physical characteristics. High reconstructed summer SSTs prior to 3000 cal. a BP—especially between 4800 and 3000 cal. a BP, indicating warm conditions in Vaigat Strait—represent the strong influence of Atlantic water, and can be regarded as a local expression of the Late-Holocene Thermal Maximum (HTM). The exact timing of the HTM varies spatially across Greenland and the North Atlantic region, ending as late as ca. 3000 cal. a BP in West Greenland and Baffin Bay [64,65]. *Thalassionema nitzschioides*—the main diatom species in warmer Atlantic waters [28,52]—reached relatively high numbers during 4800–3860 cal. a BP (Supplementary Figure S1), suggesting the relatively strong influence of Atlantic water [17]. Diatom and lithological analyses from sediment core DA00-03, from the southwestern entrance of Disko Bugt, indicate a termination of the Late-HTM between 3500 and 3100 cal. a BP [2].

Temperature records based on alkenone unsaturation from the sediments of two lakes in Kangerlussuaq, West Greenland, indicate a warm interval from 5000 to 2800 cal. a BP (Figure 4B, [61]). The Greenland Ice Sheet Project Two (GISP2) ice core from Greenland Summit also depicts a general warming from 5000 to 3500 cal. a BP (Figure 4C, [62]). Based on archaeological data, Meldgaard [66] speculates that there was a change from subarctic to arctic conditions between 4200 and 3500 cal. a BP that significantly affected the availability of human food resources. The change adversely affected the

living conditions for open water hunters, and led to the demise of the Saqqaq culture in the Disko Bugt area.

A benthic foraminiferal record from offshore of East Greenland suggests the strong influence of Atlantic Intermediate Water during the mid-Holocene, which lasted until at least 4000 cal. a BP [67]. In addition, the North Iceland shelf was strongly influenced by the IC from 4600 to 3600 cal. a BP [68]. A significant warming (ca. 3 °C) is indicated in diatom-based SST records from off the North Iceland shelf between 4300 and 4000 cal. a BP [29], and from the inner North Icelandic Shelf from 4600 to 3800 cal. a BP [68]. The strong influence of Atlantic water in the East Greenland and Icelandic regions probably also reflected an active North Atlantic Current and increased advection of IC water into the WGC system, which may in turn have influenced the hydrography and climate of the Disko Bugt region.

5.2. 3000–2000 cal. a BP: Neoglacial Cooling

A gradually decreasing trend of summer SSTs between ca. 3000 and 2000 cal. a BP highlights a strong contribution from the EGC, and hence relatively cold conditions in Vaigat Strait, with the exception of two minor warm peaks centered at 2700 and at 2300 cal. a BP (Figure 4A). The time interval from 3000 to 2000 cal. a BP is characterized by a rapid increase in the abundance of sea-ice diatom species (*Detonula confervaceae* resting spores, *Fragilariopsis cylindrus*, *Fossula arctica*, and *Thalassiosira bulbosa*), as well as *Bacterosira bathyomphala* and *Thalassiosira nordenskioeldii* (Supplementary Figure S1), which indicate a significant increase in the influence of Polar waters in Vaigat Strait [17]. The foraminiferal record from the same core also indicates colder subsurface water masses in Vaigat Strait between 3500 and 2000 cal. a BP [45]. The decrease in the reconstructed SSTs was presumably a consequence of the "Neoglacial", an interval of general Northern Hemispheric cooling, which is conventionally defined as the advance of continental glaciers following the termination of the Wisconsin glaciation during the early Holocene thermal maximum [69].

A similar scenario was recognized in western Disko Bugt, where the benthic foraminifera record from core DA00-03 indicates relatively cool bottom water conditions during the time interval from 3200 to 2200 cal. a BP. The very low abundance of Atlantic water indicators, together with intense dissolution from 2700 to 2200 cal. a BP, indicates an especially cool WGC at that time [70]. In addition, a remarkable decrease in temperatures in the records from Kangerlussuaq lake and GISP2 ice core also reflects a cooling trend from 3000 to 2000 cal. a BP (Figure 4B,C, [61,62]).

A multiproxy study in Ameralik fjord near Nuuk, SW Greenland, indicated the decreased influx of IC water at subsurface depths [71]. Likewise, data from East Greenland [67] reflecting a colder EGC, and from north Iceland [72] reflecting a reduced IC influence also indicates cold regional oceanographic conditions at that time. A diatom-based reconstruction of August SST on the northern shelf of Iceland also exhibits a decrease of ~2 °C from 3000 to 2200 cal. a BP, together with a decrease in the warm North Atlantic diatom assemblage [73]. These archives suggest that the IC decreased in strength and that an enhanced inflow of Polar water from the EGC affected the hydrography and climate in the northern North Atlantic during this interval. The neoglacial cooling was presumably forced by a reduction in solar radiation beyond a critical threshold, and was enhanced by a resulting advance of the southern margin of the Arctic drift ice along the East Greenland margin [67].

5.3. After 2000 cal. a BP:

5.3.1. 2000–1600 cal. a BP: Roman Warm Period

The reconstructed summer SSTs in Vaigat Strait during the last 2000 years indicate increasing climatic instability in Vaigat Strait. A gradual increase in summer SST occurred after 2000 cal. a BP and continued until 1600 cal. a BP, suggesting the strengthened impact of the IC, and corresponds to the so-called "Roman Warm Period" (RWP, 2300–1500 cal. a BP) [3]. This is also reflected in the diatom data by a marked increase in warm-water species and near absence of the sea-ice species

(Supplementary Figure S1, [17]). In addition, sea-surface temperature records from Disko Bugt reflect an increased influence of Atlantic surface water from ca. 2200–1700 and from 2100 to 1500 cal. a BP [1,2]. D'Andrea et al. [61] inferred a progressive warming in Kangerlussuaq lake water temperatures from 2000 to 1700 cal. a BP, and suggested that this would have adversely affected the Dorset culture, since they were mainly sea-ice hunters (Figure 4B, [61]). Dinoflagellate cyst records spanning the same time interval also suggest increased sea-surface temperatures and fewer months with sea-ice cover in the Canadian high arctic [74,75].

The "Roman Warm Period" was characterised by warmer conditions on the East Greenland shelf [67], Reykjanes Ridge [76] and to the north of Iceland [73,77]. Marine records from the Vøring Plateau [78], Barents Sea [79], and terrestrial wintertime precipitation records from maritime glaciers in northern Norway [80] suggest a warm North Atlantic Current and increased northwards moisture transport during the "Roman Warm Period".

5.3.2. 1500–1200 cal. a BP: Dark Ages Cold Period

Between 1500 and 1200 cal. a BP, there was a significant decrease in the reconstructed summer SSTs, coinciding with the disappearance of warm-water diatom taxa and significant increase in the sea-ice species *F. cylindrus* (Supplementary Figure S1, [17]). This implies an increase in the influence of cold Polar water in Vaigat Strait and a further decrease in SST, corresponding to a significant climatic deterioration in NW Europe, known as the "Dark Ages Cold Period" (DACP, ca. 1550~1150 cal. a BP; cf. [81]). Both the Kangerlussuaq lake and GISP 2 temperature records indicate a significant cooling during 1500–1200 cal. a BP (Figure 4B,C, [61,62]).

These inferences regarding summer SST variations reflected by the diatom record from Vaigat Strait are supported by dinoflagellate cyst data from core DA00-02 from Disko Bugt, which indicate a gradual decrease in warm-water taxa from 1500 to 1300 cal. a BP [3]. In addition, diatom and dinoflagellate cyst records from South Greenland indicate a cold phase during this interval related to an increased influx of EGC water, although the overall strength of the WGC seems to have increased [71]. Thus, the entire East Greenland region may have experienced an increased influx of EGC water [67]. In addition, the Canadian high arctic waters of the Nares Strait experienced surface-water cooling and more extensive sea-ice cover, indicating regional atmospheric cooling [75].

5.3.3. 1200–630 cal. a BP: Medieval Climate Anomaly

The reconstructed summer SST record reveals a warming interval from 1200 to 630 cal. a BP, interrupted by a minor cold episode centered at 840 cal. a BP, suggesting a strong influx of Atlantic surface waters to Vaigat Strait. This warm interval corresponds to the European Medieval Climate Anomaly (MCA, 1200~700 cal. a BP; [82]). The Kangerlussuaq lake water temperature record reveals a warm interval from ca. 1100 to 850 cal. a BP, coincident with Norse colonization of Greenland (Figure 4B, [61]). The GISP2 temperature record also suggests a warm interval from 1200 to 750 cal. a BP (Figure 4C, [62]).

Evidence of the MCA can be found throughout West Greenland and across the North Atlantic region. In Holsteinsborg Dyb, off West Greenland, the MCA is documented by relatively warm surface waters during the interval from 1150 to 650 cal. a BP [83]. In Igaliku Fjord, SW Greenland, Jensen et al. [10] identified an interval of increased warm-water diatom species from 1180 to 600 cal. a BP, associated with a decrease in the influx of EGC water; and Roncaglia and Kuijpers [84] identified a relatively warm interval starting at about 1180 cal. a BP based on dinoflagellate cysts.

On the East Greenland shelf between 1200 and 850 cal. a BP, the influence of Polar water was reduced, which allowed the encroachment of Atlantic Intermediate Water along the sea floor [85]. In addition, the North Icelandic shelf was dominated by Atlantic water during 1150–650 cal. a BP [19,68,86–88]. Similarly, diatom records from the central Canadian Arctic Archipelago reveal a higher species diversity around ca. 1150–600 cal. a BP, suggesting a warmer climate than either before or after [89].

5.3.4. After 630 cal. a BP: Little Ice Age

The reconstructed summer SSTs decreased rapidly in Vaigat Strait after 630 cal. a BP (Figure 4A), and warm-water diatom taxa were almost completely absent after 650 cal. a BP (Supplementary Figure S1, [17]). The GISP2 ice-core paleo-temperature record also suggests a significant cold interval after 750 cal. a BP (Figure 4C, [62]). An abrupt decrease in water temperatures of Kangerlussuaq lake began at ca. 850 cal. a BP, and cooler temperatures persisted until approximately 300 cal. a BP, except for a warmer episode centered at 500 cal. a BP (Figure 4B, [61]). We infer that this cooling event corresponds to the initiation of the "Little Ice Age" (LIA, [81]).

Although the temporal range of the LIA is not particularly well-defined in the Northern Hemisphere [90–92] and appears to be influenced significantly by location [93], the expansion of glaciers in the LIA from ca. 650 to 50 cal. a BP is well recognized across the northern hemisphere [90–92]. Ice core studies indicate decreased accumulation associated with cooling (ca. 0.5 °C) at the GISP2 Greenland Summit site centered at 750, 450, and 150 cal. a BP [94].

A change to colder hydrographic conditions caused by the increased influx of Polar water to central Disko Bugt is also indicated by the occurrence of glaciomarine foraminiferal faunas after ca. 500 cal. a BP [95]. In Igaliku Fjord, SW Greenland, decreasing diatom-inferred SSTs [10] and dinoflagellate cysts [84] reveal a cooling trend that started at 665 cal. a BP. Offshore of SE Greenland, diatom data reveal a cooling of the EGC after ca. 750 cal. a BP [10], coincident with similar indications from onshore data in the same area [96]. Furthermore, a diatom-based SST reconstruction from the North Icelandic shelf suggests a marked reduction in temperature at around 650 cal. a BP [15], caused by the significantly increased influence of Polar waters from the EGC in that area.

5.4. Links between SST Changes and Solar Activity

Correlations between paleotemperature records from the North Atlantic and solar activity suggest that changes in solar output may cause significant shifts in the climate of the North Atlantic region [97]. To test the role of solar activity on summer SST at our study site in West Greenland, we conducted a cross-correlation analysis between our reconstructed summer SST record and a total solar irradiance (TSI) series (Figure 6). The results indicate that the maximum correlation coefficient (0.284) of summer SST and TSI records is obtained at nearly zero time-lag (-6 time-lag) (Figure 6), which means that variations in solar activity affected the summer SST variability in the study area.

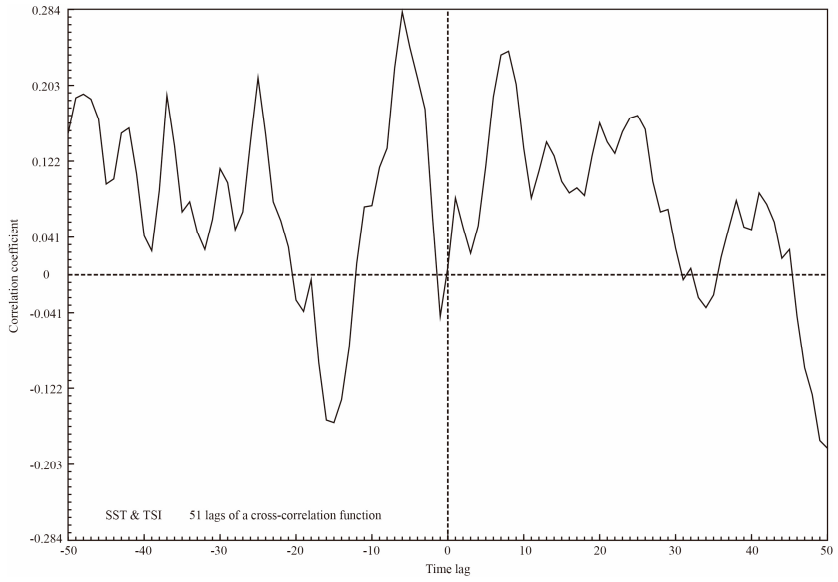

Figure 6. Results of cross-correlation analysis between the reconstructed summer SST record from Vaigat Strait and total solar irradiance (TSI) series.

A significant positive relationship between summer SSTs on the North Icelandic shelf and solar irradiance reconstructed from ^{10}Be and ^{14}C records during the Holocene was also demonstrated by Jiang et al. [15,16]. This finding is also supported by recent climate model simulations using the Community Climate System Model version 4 (CCSM4) [98]. The model results show a strong positive correlation between SST and solar irradiance in the pathway of the IC, indicating that a reduced frequency of Atlantic blocking events during periods of high solar irradiance promotes warmer and saltier conditions in the pathway of the IC due to stronger circulation of the subpolar gyre [16].

6. Conclusions

Modern diatom assemblages from 80 surface sediment samples from west of Greenland and around Iceland were used to establish a new diatom-based transfer function for reconstructing summer sea-surface temperature (SST). A gradual decrease in summer SSTs recorded in core DA06-139G reflects a cooling trend, with several fluctuations superimposed, during the last 5000 years in Vaigat Strait in Disko Bugt.

The reconstructed summer SST record ranges from 1.4 to 5 °C, with a mean of 3.1 °C. Summer SSTs were generally higher than the mean before 3000 cal. a BP, which is correlative with the Late-Holocene Thermal Maximum. There followed a step-by-step decrease in summer SSTs between 3000 and 2000 cal. a BP, known as the "Neoglacial cooling". After 2000 cal. a BP, two cooling events at 1500–1200 cal. a BP and 630–50 cal. a BP are distinguished in the summer SST record, as well as two significantly warm episodes from 2000 to 1600 cal. a BP and from 1200 to 630 cal. a BP. Comparison of the summer SST record from Vaigat Strait with reconstructed temperatures at Kangerlussuaq lake, West Greenland, and the GISP2 ice core reveals coherent changes and a consistent pattern of variation, reflecting regional changes in SST in West Greenland.

Spectral analyses indicate that significant centennial-scale variations are superimposed on the long-term orbital trend. The dominant periodicities are 529, 410, and 191 years, which may be linked to the well-known 512- and 206-year solar cycles. Cross-correlation analyses between the summer SSTs and total solar irradiance through the last 5000 years indicate that the records are in phase, providing evidence that variations in solar activity impacted regional summer SST variability. Overall, the strong linkage between solar variability and summer SSTs is not only of regional significance, but is also consistent over the entire North Atlantic region.

Supplementary Materials: The following are available online at www.mdpi.com/2071-1050/9/5/704/s1, Figure S1: Relative abundance (%) of the distribution (excluding Chaetoceros resting spores) of the most common diatoms in the studied record of core DA06-139G [17], Table S1: Location and water depth (m) of surface samples.

Acknowledgments: Core DA06-139G was collected in 2006 during a cruise of RV Dana funded by GEUS, the Bureau of Mineral Resources in Nuuk, and NunaOil, Greenland. We thank the captain and crew for their engagement during the work at sea, and John Boserup (GEUS, Øster Voldgade 10, DK-1350 Copenhagen K, Denmark) for assisting with sediment coring. Kaarina Weckström and Camilla S. Andresen are also acknowledged for sharing their data. We acknowledge financial support from the National Natural Science Foundation of China (grants 41406209, 41302134, U1609203), the Natural Science Foundation of Zhejiang Province (grant LY17D060001), the Chinese polar environment comprehensive investigation & assessment programs (Grant CHINARE2017-03-02) and the K. C. Wong Magna Fund of Ningbo University.

Author Contributions: Dongling Li, Longbin Sha and Hui Jiang conceived and designed the experiments; Yanni Wu performed the experiments; Dongling Li and Longbin Sha analysed the data; All authors contributed to data interpretation; Dongling Li, Longbin Sha and Hui Jiang wrote the paper with significant input from Jialin Li and Yanguang Liu.

Conflicts of Interest: The authors declare no conflict of interest.

References

1. Lloyd, J.M.; Park, L.A.; Kuijpers, A.; Moros, M. Early Holocene palaeoceanography and deglacial chronology of Disko Bugt, West Greenland. *Quat. Sci. Rev.* **2005**, *24*, 1741–1755. [CrossRef]
2. Moros, M.; Jensen, K.G.; Kuijpers, A. Mid-to late-Holocene hydrological and climatic variability in Disko Bugt, central West Greenland. *Holocene* **2006**, *16*, 357–367. [CrossRef]

3. Seidenkrantz, M.-S.; Roncaglia, L.; Fischel, A.; Moros, M. Variable North Atlantic climate seesaw patterns documented by a late Holocene marine record from Disko Bugt, West Greenland. *Mar. Micropaleontol.* **2008**, *68*, 66–83. [CrossRef]
4. Krawczyk, D.W.; Witkowski, A.; Moros, M.; Lloyd, J.M.; Kuijpers, A.; Kierzek, A. Late-Holocene diatom-inferred reconstruction of temperature variations of the West Greenland Current from Disko Bugt, central West Greenland. *Holocene* **2010**, *20*, 659–666. [CrossRef]
5. Joughin, I.; Abdalati, W.; Fahnestock, M. Large fluctuations in speed on Greenland's Jakobshavn Isbræ glacier. *Nature* **2004**, *432*, 608–610. [CrossRef] [PubMed]
6. Joughin, I. Greenland Rumbles Louder as Glaciers Accelerate. *Science* **2006**, *311*, 1719–1720. [CrossRef] [PubMed]
7. Joughin, I.; Das, S.B.; King, M.A.; Smith, B.E.; Howat, I.M.; Moon, T. Seasonal speedup along the western flank of the Greenland ice sheet. *Science* **2008**, *320*, 781–783. [CrossRef] [PubMed]
8. Rignot, E.; Kanagaratnam, P. Changes in the velocity structure of the Greenland Ice Sheet. *Science* **2006**, *311*, 986–990. [CrossRef] [PubMed]
9. Moros, M.; Lloyd, J.M.; Perner, K.; Krawczyk, D.; Blanz, T.; de Vernal, A.; Ouellet-Bernier, M.M.; Kuijpers, A.; Jennings, A.E.; Witkowski, A.; et al. Surface and sub-surface multi-proxy reconstruction of middle to late Holocene palaeoceanographic changes in Disko Bugt, West Greenland. *Quat. Sci. Rev.* **2016**, *132*, 146–160. [CrossRef]
10. Jensen, K.G.; Kuijpers, A.; Koç, N.; Heinemeier, J. Diatom evidence of hydrographic changes and ice conditions in Igaliku Fjord, South Greenland, during the past 1500 years. *Holocene* **2004**, *14*, 152–164. [CrossRef]
11. Ren, J.; Jiang, H.; Seidenkrantz, M.-S.; Kuijpers, A. A diatom-based reconstruction of Early Holocene hydrographic and climatic change in a southwest Greenland fjord. *Mar. Micropaleontol.* **2009**, *70*, 166–176. [CrossRef]
12. Berner, K.S.; Koç, N.; Divine, D.; Godtliebsen, F.; Moros, M. A decadal-scale Holocene sea surface temperature record from the subpolar North Atlantic constructed using diatoms and statistics and its relation to other climate parameters. *Paleoceanography* **2008**, *23*, PA2210. [CrossRef]
13. Sicre, M.-A.; Hall, I.R.; Mignot, J.; Khodri, M.; Ezat, U.; Truong, M.X.; Eiríksson, J.; Knudsen, K.L. Sea surface temperature variability in the subpolar Atlantic over the last two millennia. *Paleoceanography* **2011**, *26*, PA4218. [CrossRef]
14. Sicre, M.-A.; Weckström, K.; Seidenkrantz, M.S.; Kuijpers, A.; Benetti, M.; Masse, G.; Ezat, U.; Schmidt, S.; Bouloubassi, I.; Olsen, J.; et al. Labrador current variability over the last 2000 years. *Earth Planet. Sci. Lett.* **2014**, *400*, 26–32. [CrossRef]
15. Jiang, H.; Eiríksson, J.; Schulz, M.; Knudsen, K.L.; Seidenkrantz, M.-S. Evidence for solar forcing of sea-surface temperature on the North Icelandic Shelf during the late Holocene. *Geology* **2005**, *33*, 73–76. [CrossRef]
16. Jiang, H.; Muscheler, R.; Björck, S.; Seidenkrantz, M.-S.; Olsen, J.; Sha, L. Solar forcing of Holocene summer sea-surface temperatures in the northern North Atlantic. *Geology* **2015**, *43*, 203–206. [CrossRef]
17. Sha, L.; Jiang, H.; Seidenkrantz, M.-S.; Knudsen, K.L.; Olsen, J.; Kuijpers, A.; Liu, Y. A diatom-based sea-ice reconstruction for the Vaigat Strait (Disko Bugt, West Greenland) over the last 5000 yr. *Palaeogeogr. Palaeoclimatol. Palaeoecol.* **2014**, *403*, 66–79. [CrossRef]
18. Sha, L.; Jiang, H.; Seidenkrantz, M.-S.; Muscheler, R.; Zhang, X.; Knudsen, M.F.; Olsen, J.; Knudsen, K.L.; Zhang, W. Solar forcing as an important trigger for West Greenland sea-ice variability over the last millennium. *Quat. Sci. Rev.* **2016**, *131*, 148–156. [CrossRef]
19. Ran, L.; Jiang, H.; Knudsen, K.L.; Eiríksson, J. Diatom-based reconstruction of palaeoceanographic changes on the North Icelandic shelf during the last millennium. *Palaeogeogr. Palaeoclimatol. Palaeoecol.* **2011**, *302*, 109–119. [CrossRef]
20. Rigual-Hernández, A.S.; Colmenero-Hidalgo, E.; Martrat, B.; Bárcena, M.A.; de Vernal, A.; Sierro, F.J.; Flores, J.A.; Grimalt, J.O.; Henry, M.; Lucchi, R.G. Svalbard ice-sheet decay after the Last Glacial Maximum: New insights from micropalaeontological and organic biomarker paleoceanographical reconstructions. *Palaeogeogr. Palaeoclimatol. Palaeoecol.* **2017**, *465*, 225–236. [CrossRef]
21. Carbonara, K.; Mezgec, K.; Varagona, G.; Musco, M.E.; Lucchi, R.G.; Villa, G.; Morigi, C.; Melis, R.; Caffau, M. Palaeoclimatic changes in Kveithola, Svalbard, during the Late Pleistocene deglaciation and Holocene:

Evidences from microfossil and sedimentary records. *Palaeogeogr. Palaeoclimatol. Palaeoecol.* **2016**, *463*, 136–149. [CrossRef]
22. Berner, K.S.; Koç, N.; Godtliebsen, F.; Divine, D.V. Holocene climate variability of the Norwegian Atlantic Current during high and low solar insolation forcing. *Paleoceanography* **2011**, *26*, 252–257. [CrossRef]
23. Miettinen, A.; Divine, D.; Koç, N.; Godtliebsen, F.; Hall, I.R. Multicentennial Variability of the Sea Surface Temperature Gradient across the Subpolar North Atlantic over the Last 2.8 kyr. *J. Clim.* **2012**, *25*, 4205–4219. [CrossRef]
24. Miettinen, A.; Divine, D.; Husum, K.; Koç, N.; Jennings, A.E. Exceptional ocean surface conditions on the SE Greenland shelf during the Medieval Climate Anomaly. *Paleoceanography* **2015**, *30*, 1657–1674. [CrossRef]
25. Hasle, G.R.; Syvertsen, E.E. Marine diatoms. In *Identifying Marine Phytoplankton*; Tomas, C.R., Ed.; Academic Press Inc.: San Diego, CA, USA, 1997; pp. 5–385.
26. Von Quillfeldt, C.H. Identification of Some Easily Confused Common Diatom Species in Arctic Spring Blooms. *Bot. Mar.* **2001**, *44*, 375–389. [CrossRef]
27. Arrigo, K.R.; Perovich, D.K.; Pickart, R.S.; Brown, Z.W.; van Dijken, G.L.; Lowry, K.E.; Mills, M.M.; Palmer, M.A.; Balch, W.M.; Bahr, F.; et al. Massive phytoplankton blooms under Arctic sea ice. *Science* **2012**, *336*, 1408. [CrossRef] [PubMed]
28. Jiang, H.; Seidenkrantz, M.-S.; Knudsen, K.L.; Eiriksson, J. Diatom surface sediment assemblages around Iceland and their relationships to oceanic environmental variables. *Mar. Micropaleontol.* **2001**, *41*, 73–96. [CrossRef]
29. Andersen, C. Nonuniform response of the major surface currents in the Nordic Seas to insolation forcing: Implications for the Holocene climate variability. *Paleoceanography* **2004**, *19*, 1–16. [CrossRef]
30. Andersen, C.; Koç, N.; Moros, M. A highly unstable Holocene climate in the subpolar North Atlantic: Evidence from diatoms. *Quat. Sci. Rev.* **2004**, *23*, 2155–2166. [CrossRef]
31. Krawczyk, D.W.; Witkowski, A.; Moros, M.; Lloyd, J.M.; Høyer, J.L.; Miettinen, A.; Kuijpers, A. Quantitative reconstruction of Holocene sea ice and sea surface temperature off West Greenland from the first regional diatom data set. *Paleoceanography* **2017**, *31*, 18–40. [CrossRef]
32. Steinhilber, F.; Beer, J.; Fröhlich, C. Total solar irradiance during the Holocene. *Geophys. Res. Lett.* **2009**, *36*, LP19704. [CrossRef]
33. Kodera, K.; Kuroda, Y. Dynamical response to the solar cycle. *J. Geophys. Res.* **2002**, *107*, ACL 5-1–ACL 5-12. [CrossRef]
34. Ruzmaikin, A.; Feynman, J.; Jiang, X.; Noone, D.C.; Waple, A.M.; Yung, Y.L. The pattern of northern hemisphere surface air temperature during prolonged periods of low solar output. *Geophys. Res. Lett.* **2004**, *31*, 261–268. [CrossRef]
35. Haigh, J.D.; Roscoe, H.K. Solar influences on polar modes of variability. *Meteorol. Z.* **2006**, *15*, 371–378. [CrossRef]
36. Hodell, D.A.; Kanfoush, S.L.; Shemesh, A.; Crosta, X.; Charles, C.D.; Guilderson, T.P. Abrupt Cooling of Antarctic Surface Waters and Sea Ice Expansion in the South Atlantic Sector of the Southern Ocean at 5000 cal yr B.P. *Quat. Res.* **2001**, *56*, 191–198. [CrossRef]
37. Knudsen, M.F.; Jacobsen, B.H.; Seidenkrantz, M.-S.; Olsen, J. Evidence for external forcing of the Atlantic Multidecadal Oscillation since termination of the Little Ice Age. *Nat. Commun.* **2014**, *5*, 3323. [CrossRef] [PubMed]
38. Marchitto, T.M.; Muscheler, R.; Ortiz, J.D.; Carriquiry, J.D.; van Geen, A. Dynamical Response of the Tropical Pacific Ocean to Solar Forcing During the Early Holocene. *Science* **2010**, *330*, 1378–1381. [CrossRef] [PubMed]
39. Martin-Puertas, C.; Matthes, K.; Brauer, A.; Muscheler, R.; Hansen, F.; Petrick, C.; Aldahan, A.; Possnert, G.; van Geel, B. Regional atmospheric circulation shifts induced by a grand solar minimum. *Nat. Geosci.* **2012**, *5*, 397–401. [CrossRef]
40. Verschuren, D.; Laird, K.R.; Cumming, B.F. Rainfall and drought in equatorial east Africa during the past 1100 years. *Nature* **2000**, *403*, 410–414. [CrossRef] [PubMed]
41. Bond, G.; Kromer, B.; Beer, J.; Muscheler, R.; Evans, M.N.; Showers, W.; Hoffmann, S.; Lotti-Bond, R.; Hajdas, I.; Bonani, G. Persistent solar influence on North Atlantic climate during the Holocene. *Science* **2001**, *294*, 2130–2136. [CrossRef] [PubMed]
42. Holzhauser, H.; Magny, M.J.; Zumbuuhl, H.J. Glacier and lake-level variations in west-central Europe over the last 3500 years. *Holocene* **2005**, *15*, 789–801. [CrossRef]

43. Sejrup, H.P.; Lehman, S.J.; Haflidason, H.; Noone, D.; Muscheler, R.; Berstad, I.M.; Andrews, J.T. Response of Norwegian Sea temperature to solar forcing since 1000 A.D. *J. Geophys. Res.* **2010**, *115*, 168–172. [CrossRef]
44. Long, A.J.; Roberts, D.H. Late Weichselian deglacial history of Disko Bugt, West Greenland, and the dynamics of the Jakobshavns Isbrae ice stream. *Boreas* **2003**, *32*, 208–226. [CrossRef]
45. Andresen, C.S.; McCarthy, D.; Valdemar Dylmer, C.; Lloyd, J.M. Interaction between subsurface ocean waters and calving of the Jakobshavn Isbræ during the late Holocene. *Holocene* **2011**, *21*, 211–224. [CrossRef]
46. Weidick, A.; Bennike, O. Quaternary glaciation history and glaciology of Jakobshavn Isbræ and the Disko Bugt region, West Greenland: A review. *Geol. Surv. Den. Greenl.* **2007**, *14*, 78.
47. Buch, E. Review of oceanographic conditions in subarea 0 and 1 during the 1970–79 decade. *NAFO Sci. Coun. Stud.* **1982**, *5*, 43–50.
48. Tang, C.C.L.; Ross, C.K.; Yao, T.; Petrie, B.; DeTracey, B.M.; Dunlap, E. The circulation, water masses and sea-ice of Baffin Bay. *Prog. Oceanogr.* **2004**, *63*, 183–228. [CrossRef]
49. Andersen, O.G.N. The annual cycle of phytoplankton primary production and hydrography in the Disko Bugt area, West Greenland. *Meddelelser om Grønland Biosci.* **1981**, *6*, 68.
50. Dalhoff, F.; Kuijpers, A. *Havbunds Prøveindsamling ud for Vest Grønland 2006. RV Dana Cruise Report*; Danmarks og Grønlands Geologiske Undersøgelse: Copenhagen, Denmark, 2007.
51. Håkansson, H. The recent diatom succession of Lake Havgårdssjön, South Sweden. In Proceedings of the Seventh International Diatom Symposium, Philadelphia, PA, USA, 22–27 August 1982; Mann, D.G., Ed.; Otto Koeltz Science Publishers: Koenigstein, Germany, 1984; pp. 411–429.
52. Koç Karpuz, N.; Schrader, H. Surface sediment diatom distribution and Holocene paleotemperature variations in the Greenland, Iceland and Norwegian Sea. *Paleoceanography* **1990**, *5*, 557–580. [CrossRef]
53. Cremer, H. Distribution patterns of diatom surface sediment assemblages in the Laptev Sea (Arctic Ocean). *Mar. Micropaleontol.* **1999**, *38*, 39–67. [CrossRef]
54. Ramsey, C.B. Deposition models for chronological records. *Quat. Sci. Rev.* **2008**, *27*, 42–60. [CrossRef]
55. Reimer, P.J.; Baillie, M.G.L.; Bard, E.; Bayliss, A.; Beck, J.W.; Blackwell, P.G.; Bronk Ramsey, C.; Buck, C.E.; Burr, G.S.; Edwards, R.L.; et al. IntCal09 and Marine09 radiocarbon age calibration curves, 0–50,000 years cal BP. *Radiocarbon* **2009**, *51*, 1111–1150. [CrossRef]
56. McNeely, R.; Dyke, A.S.; Southon, J.R. Canadian Marine Reservoir Ages, Preliminary Data Assessment, Open File 5049: 3. Geological Survey Canada [WWW Document]. Available online: http://geopub.nrcan.gc.ca (accessed on 27 April 2017).
57. Lloyd, J.M.; Moros, M.; Perner, K.; Telford, R.J.; Kuijpers, A.; Jansen, E.; McCarthy, D. A 100 years record of ocean temperature control on the stability of Jakobshavn Isbrae, West Greenland. *Geology* **2011**, *39*, 867–870. [CrossRef]
58. Juggins, S. *C2 User Guide: Software for Ecological and Palaeoecological Data Analysis and Visualisation, Version 1.5*; Newcastle University: Newcastle upon Tyne, UK, 2003.
59. Schulz, M. REDFIT: Estimating red-noise spectra directly from unevenly spaced paleoclimatic time series. *Comput. Geosci.* **2002**, *28*, 421–426. [CrossRef]
60. Howell, P.; Pisias, N.; Balance, J.; Baughman, J.; Ochs, L. *ARAND Time-Series Analysis Software*; Brown University: Providence, RI, USA, 2006.
61. D'Andrea, W.J.; Huang, Y.; Fritz, S.C.; Anderson, N.J. Abrupt Holocene climate change as an important factor for human migration in West Greenland. *Proc. Natl. Acad. Sci. USA* **2011**, *108*, 9765–9769.
62. Alley, R.B. *GISP2 Ice Core Temperature and Accumulation Data*; National Oceanic and Atmospheric Administration/National Geophysical Data Center Paleoclimatology Program: Boulder, CO, USA, 2004.
63. Stuiver, M.; Braziunas, T.F. Sun, ocean, climate and atmospheric $^{14}CO_2$: An evaluation of causal and spectral relationships. *Holocene* **1993**, *3*, 289–305. [CrossRef]
64. Kaufman, D.S.; Ager, T.A.; Anderson, N.J.; Wolfe, B.B. Holocene thermal maximum in the western Arctic (0–180°W). *Quat. Sci. Rev.* **2004**, *23*, 529–560. [CrossRef]
65. Kaplan, M.R.; Wolfe, A.P.; Miller, G.H. Holocene environmental variability in Southern Greenland inferred from lake sediments. *Quat. Res.* **2002**, *58*, 149–159. [CrossRef]
66. Meldgaard, M. Ancient Harp Seal hunters of Disko Bay. Subsistence and settlement at the Saqqaq culture site Qeqertasussuk (2400/1400 BC), West Greenland. *Meddelelser om Grønland Man Soc.* **2004**, *30*, 189.
67. Jennings, A.E.; Knudsen, K.L.; Hald, M.; Hansen, C.V.; Andrews, J.T. A mid-Holocene shift in Arctic sea-ice variability on the East Greenland Shelf. *Holocene* **2002**, *12*, 49–58. [CrossRef]

68. Jiang, H.; Seidenkrantz, M.-S.; Knudsen, K.L.; Eiríksson, J. Late-Holocene summer sea-surface temperatures based on a diatom record from the north Icelandic shelf. *Holocene* **2002**, *12*, 137–147. [CrossRef]
69. Porter, S.C.; Denton, G.H. Chronology of neoglaciation in the North American Cordillera. *Am. J. Sci.* **1967**, *265*, 177–210. [CrossRef]
70. Lloyd, J.M.; Kuijpers, A.; Long, A.; Moros, M.; Park, L.A. Foraminiferal reconstruction of mid- to late-Holocene ocean circulation and climate variability in Disko Bugt, West Greenland. *Holocene* **2007**, *17*, 1079–1091. [CrossRef]
71. Seidenkrantz, M.-S.; Aagaard-Sørensen, S.; Sulsbrück, H.; Kuijpers, A.; Jensen, K.G.; Kunzendorf, H. Hydrography and climate of the last 4400 years in a SW Greenland fjord: Implications for Labrador Sea palaeoceanography. *Holocene* **2007**, *17*, 387–401. [CrossRef]
72. Andrews, J.T.; Caseldine, C.; Weiner, N.J.; Hatton, J. Late Holocene (ca. 4 ka) marine and terrestrial environmental change in Reykjarfjördur, north Iceland: Climate and/or settlement? *J. Quat. Sci.* **2001**, *16*, 133–143. [CrossRef]
73. Justwan, A.; Koç, N.; Jennings, A.E. Evolution of the Irminger and East Icelandic Current systems through the Holocene, revealed by diatom-based sea surface temperature reconstructions. *Quat. Sci. Rev.* **2008**, *27*, 1571–1582. [CrossRef]
74. Mudie, P.J.; Rochon, A.; Levac, E. Decadal-scale sea ice changes in the Canadian Arctic and their impacts on humans during the past 4000 years. *Environ. Archaeol.* **2005**, *10*, 113–126. [CrossRef]
75. Mudie, P.J.; Rochon, A.; Prins, M.A.; Soenarjo, D.; Troelstra, S.R.; Levac, E.; Scott, D.B.; Roncaglia, L.; Kuijpers, A. Late Pleistocene-Holocene marine geology of Nares Strait Region: Palaeoceanography from foraminifera and dinoflagellate cysts, sedimentology and stable. *Polarforschung* **2006**, *74*, 169–183.
76. Moros, M.; Jansen, E.; Oppo, D.W.; Giraudeau, J.; Kuijpers, A. Reconstruction of the late-Holocene changes in the Sub-Arctic Front position at the Reykjanes Ridge, north Atlantic. *Holocene* **2012**, *22*, 877–886. [CrossRef]
77. Andrews, J.T.; Giraudeau, J. Multi-proxy records showing significant Holocene environmental variability: The inner N. Iceland shelf (Húnaflói). *Quat. Sci. Rev.* **2003**, *22*, 175–193. [CrossRef]
78. Risebrobakken, B.; Jansen, E.; Andersson, C.; Mjelde, E.; Hevrøy, K. A high-resolution study of Holocene paleoclimatic and paleoceanographic changes in the Nordic Seas. *Paleoceanography* **2003**, *18*, 123–126. [CrossRef]
79. Sarnthein, M.; van Kreveld, S.; Erlenkeuser, H.; Grootes, P.M.; Kucera, M.; Pflaumann, U.; Schulz, M. Centennial-to-millennial-scale periodicities of Holocene climate and sediment injections off the western Barents shelf, 75°N. *Boreas* **2003**, *32*, 447–461. [CrossRef]
80. Bakke, J.; Lie, Ø.; Dahl, S.O.; Nesje, A.; Bjune, A.E. Strength and spatial patterns of the Holocene wintertime westerlies in the NE Atlantic region. *Glob. Planet. Chang.* **2008**, *60*, 28–41. [CrossRef]
81. Lamb, H.H. *Climate, History and the Modern World*; Routledge: New York, NY, USA, 1995.
82. Mann, M.E.; Zhang, Z.; Rutherford, S.; Bradley, R.S.; Hughes, M.K.; Shindell, D.; Ammann, C.; Faluvegi, G.; Ni, F. Global signatures and dynamical origins of the Little Ice Age and Medieval Climate Anomaly. *Science* **2009**, *326*, 1256–1260. [CrossRef] [PubMed]
83. Sha, L.; Jiang, H.; Knudsen, K.L. Diatom evidence of climatic change in Holsteinsborg Dyb, west of Greenland, during the last 1200 years. *Holocene* **2012**, *22*, 347–358. [CrossRef]
84. Roncaglia, L.; Kuijpers, A. Palynofacies analysis and organic-walled dinoflagellate cysts in late-Holocene sediments from Igaliku Fjord, South Greenland. *Holocene* **2004**, *14*, 172–184. [CrossRef]
85. Jennings, A.E.; Weiner, N.J. Environmental change in eastern Greenland during the last 1300 years: Evidence from foraminifera and lithologies in Nansen Fjord, 68°N. *Holocene* **1996**, *6*, 179–191. [CrossRef]
86. Eiríksson, J.; Knudsen, K.L.; Haflidason, H.; Henriksen, P. Late-glacial and Holocene palaeoceanography of the North Icelandic shelf. *J. Quat. Sci.* **2000**, *15*, 23–42. [CrossRef]
87. Knudsen, K.L.; Eiríksson, J.; Jansen, E.; Jiang, H.; Rytter, F.; Gudmundsdóttir, E.R. Palaeoceanographic changes off North Iceland through the last 1200 years: Foraminifera, stable isotopes, diatoms and ice rafted debris. *Quat. Sci. Rev.* **2004**, *23*, 2231–2246. [CrossRef]
88. Knudsen, K.L.; Eiríksson, J.; Bartels-Jónsdóttir, H.B. Oceanographic changes through the last millennium off North Iceland: Temperature and salinity reconstructions based on foraminifera and stable isotopes. *Mar. Micropaleontol.* **2012**, *84*, 54–73. [CrossRef]
89. LeBlanc, M.; Gajewski, K.; Hamilton, P.B. A diatom-based Holocene palaeoenvironmental record from a mid-arctic lake on Boothia Peninsula, Nunavut, Canada. *Holocene* **2004**, *14*, 417–425. [CrossRef]

90. Grove, J.M. *The Little Ice Age*; Routledge: New York, NY, USA, 1988.
91. Grove, J.M. The initiation of the "Little Ice Age" in regions round the North Atlantic. *Clim. Chang.* **2001**, *48*, 53–82. [CrossRef]
92. Broecker, W.S. Was a change in thermohaline circulation responsible for the Little Ice Age? *Proc. Natl. Acad. Sci. USA* **2000**, *97*, 1339–1342. [CrossRef] [PubMed]
93. Mayewski, P.A.; Rohling, E.E.; Stager, J.C.; Maasch, K.A.; Meeker, L.D.; Meyerson, E.A.; Gasse, F.; Kreveld, S.V.; Holmogren, K.; Lee-Thorp, J.; et al. Holocene climate variability. *Quat. Res.* **2004**, *62*, 243–255. [CrossRef]
94. Dahl-Jensen, D.; Mosegaard, K.; Gundestrup, N.; Clow, G.D.; Johnsen, S.J.; Hansen, A.W.; Balling, N. Past temperatures directly from the Greenland Ice Sheet. *Science* **1998**, *282*, 268–271. [CrossRef] [PubMed]
95. Lloyd, J.M. Late Holocene environmental change in Disko Bugt, west Greenland: Interaction between climate, ocean circulation and Jakobshavn Isbrae. *Boreas* **2006**, *35*, 35–49. [CrossRef]
96. Wagner, B.; Melles, M.; Hahne, J.; Niessen, F.; Hubberten, H.-W. Holocene climate history of Geographical Society Ø, East Greenland-evidence from lake sediments. *Palaeogeogr. Palaeoclimatol. Palaeoecol.* **2000**, *160*, 45–68. [CrossRef]
97. Bianchi, G.G.; McCave, I.N. Holocene periodicity in North Atlantic climate and deep-ocean flow south of Iceland. *Nature* **1999**, *397*, 515–517. [CrossRef]
98. Moffa-Sánchez, P.; Born, A.; Hall, I.R.; Thornalley, D.J.R.; Barker, S. Solar forcing of North Atlantic surface temperature and salinity over the past millennium. *Nat. Geosci.* **2014**, *7*, 275–278. [CrossRef]